2004

Evolution dynamics of a dense frozen Rydberg gas to plasma

Wenhui Li

Michael W. Noel
Bryn Mawr College, mnoel@brynmawr.edu

Michael P. Robinson

Paul J. Tanner

Thomas F. Gallagher

See next page for additional authors

Custom Citation

Wenhui Li, Michael W. Noel, Michael P. Robinson, Paul J. Tanner, Thomas F. Gallagher, Daniel Comparat, Bruno Laburthe Tolra, Nicolas Vanhaecke, Thibault Vogt, Nassim Zahzam, Pierre Pillet, and Duncan A. Tate, "Evolution dynamics of a dense frozen Rydberg gas to plasma," Phys. Rev. A, 70, 042713 (2004).

Authors

Wenhui Li, Michael W. Noel, Michael P. Robinson, Paul J. Tanner, Thomas F. Gallagher, Daniel Comparat, Bruno Laburthe Tolra, Nicolas Vanhaecke, Thibault Vogt, Nassim Zahzam, Pierre Pillet, and Duncan A. Tate

Evolution dynamics of a dense frozen Rydberg gas to plasma

Wenhui Li, Michael W. Noel,* Michael P. Robinson,† Paul J. Tanner, and Thomas F. Gallagher
Department of Physics, University of Virginia, McCormick Road, Charlottesville, Virginia 22903, USA

Daniel Comparat, Bruno Laburthe Tolra,‡ Nicolas Vanhaecke,§ Thibault Vogt, Nassim Zahzam, and Pierre Pillet
Laboratoire Aimé Cotton, CNRS II Campus d'Orsay, 91405 Orsay Cedex, France

Duncan A. Tate‖
Department of Physics and Astronomy, Colby College, Waterville, Maine 04901, USA

Dense samples of cold Rydberg atoms have previously been observed to spontaneously evolve to a plasma, despite the fact that each atom may be bound by as much as 100 cm^{-1}. Initially, ionization is caused by blackbody photoionization and Rydberg-Rydberg collisions. After the first electrons leave the interaction region, the net positive charge traps subsequent electrons. As a result, rapid ionization starts to occur after 1 μs caused by electron-Rydberg collisions. The resulting cold plasma expands slowly and persists for tens of microseconds. While the initial report on this process identified the key issues described above, it failed to resolve one key aspect of the evolution process. Specifically, redistribution of population to Rydberg states other than the one initially populated was not observed, a necessary mechanism to maintain the energy balance in the system. Here we report new and expanded observations showing such redistribution and confirming theoretical predictions concerning the evolution to a plasma. These measurements also indicate that, for high n states of purely cold Rydberg samples, the initial ionization process which leads to electron trapping is one involving the interactions between Rydberg atoms.

I. INTRODUCTION

For most plasmas, the lowest possible temperature is that at which there are enough energetic electrons to ionize neutral atoms to replenish the ions and electrons lost to the walls. Since electron energies of at least 5 eV (55 000 K) are required for impact ionization, it is not surprising that a 10 000 K plasma is considered a cold plasma. While ultracold one-component plasmas have been studied for some time, it was not until five years ago that the first nearly neutral ultracold plasmas were reported [1]. Such a plasma can be created by photoionization of atoms in a magneto-optical trap (MOT) using a pulsed laser. The initial observation of this phenomenon was made using 50 μK Xe atoms, but since then similar results have been found using cold Rb, Cs, and Sr atoms [2–5]. To a very good approximation, the initial electron energy is determined by the excess photon energy above the ionization limit of the photoionizing laser, while the initial positive ion temperature is that of the initially trapped atoms before ionization. After a first burst of photo-

electrons leaves the initial laser-atom interaction region, the excess positive charge of the ions traps the remaining electrons, forming the plasma. Electron collisions rapidly, on a nanosecond time scale, thermalize the electrons, typically to temperatures of tens of K, which is an extraordinarily cold plasma. A variety of fascinating phenomena has been observed in these initially well characterized plasmas, including the expansion of the plasma and recombination to form Rydberg atoms, both of which occur on the time scale of tens of microseconds [6,7]. The fact that such clean experiments can be done has stimulated theoretical interest, and many theoretical papers on the subject have appeared [8–13].

Soon after the creation of an ultracold plasma was reported, a related phenomenon was observed. Cold atoms in a MOT excited to Rydberg states of principal quantum number with $n > 30$, were found to evolve spontaneously to plasma on a time scale of ~ 1 μs, provided that the sample contained $\sim 1\%$ of hot (~ 300 K) Rydberg atoms [14]. Soon after this work, a sample of purely cold Rydberg atoms was observed to ionize spontaneously, and electron emission from such a sample was observed for more than 20 ms after the excitation of the initial Rydberg state [15]. A similar phenomenon had been observed previously in a thermal sample of cesium Rydberg atoms by Vitrant *et al.* [16] at a density a factor of 10^4 higher than those used in Refs. [14] and [15]. The evolution of the cold Rydberg atoms into the plasma was described by the following scenario. Immediately after laser excitation, cold (~ 1 mK) Rydberg atoms are photoionized by blackbody radiation and collisionally ionized by hot Rydberg atoms. The electrons produced leave the MOT volume, but the cold ions remain. Just as in the Xe ultracold plasma experiment, when enough ions accumulate, their macroscopic

charge traps subsequently produced electrons, which oscillate back and forth through the cloud of Rydberg atoms, rapidly ionizing them. (This latter behavior has been termed the "avalanche" regime.) A feature of the experiments which was not understood at the time was that population seemed to be localized in either the initially excited Rydberg state or in the plasma, whereas one would expect electron collisions with Rydberg atoms to lead to an essentially continuous distribution of final n states. The lack of other final states also raised the question of the source of the energy to create the plasma. In a state of $n=30$, the Rydberg electron is bound by 100 cm^{-1}, while in the plasma it is essentially free. What is the source of the energy?

To answer the above questions and to clarify the mechanisms by which the initial ionization occurs, we have conducted extensive systematic experiments, which we report here. Our findings confirm certain theoretical predictions concerning the evolution of a cold Rydberg sample [9], and also agree with another recent experimental paper that reports similar results [17]. (However, we studied both the preavalanche and avalanche behaviors of the evolution process, whereas Ref. [17] reports only on mechanisms during the avalanche process.)

II. EXPERIMENTAL APPROACH

The experiments reported here were performed both at the University of Virginia, using rubidium, and at Laboratoire Aimé Cotton, using cesium. In both laboratories, experiments take place in a vapor-cell MOT capable of trapping of order 10^7 atoms in the Rb $5p_{3/2}$ state or the Cs $6p_{3/2}$ state in spherical volumes that have a diameter of approximately 1 mm. Differences in the diode laser systems and anti-Helmholtz magnetic field coil geometries between the two laboratories, and also the use of different atoms, result in slightly different atom temperatures: $T=300$ μK for Rb and $T=140$ μK for Cs. Rubidium atoms in the $5p_{3/2}$ state are excited to ns or nd Rydberg states using a Littman-type pulsed dye laser with a 20 Hz repetition rate and wavelengths near 480 nm, while cesium ns and nd Rydberg atoms are excited from the $6p_{3/2}$ state using a similar dye laser system at a 10 Hz rate and a wavelength of 520 nm. For both dye laser systems, the laser pulses are 7 ns in duration, have a bandwidth of 0.3 cm^{-1}, and an energy of 100 μJ. At the University of Virginia (Rb data), the laser beam is focused into the trapped atom cloud to a diameter of 0.2 mm, thus exciting up to 10^5 Rydberg atoms in a cylindrical volume of length 1 mm and diameter 0.2 mm in each laser shot. At Laboratoire Aimé Cotton (Cs data), the diameter of the atom cloud is 0.6 mm, and the dye laser beam is focused to this same waist size. In normal trap operation, there are always some hot atoms in the Rb $5p_{3/2}$ state or Cs $6p_{3/2}$ state as a consequence of thermal (300 K) atoms passing through the MOT beams. These will also be excited to Rydberg states since the dye laser bandwidth is much greater than the Doppler width for such atoms, leading to approximately 1% of the Rydberg atoms in our sample being hot. In some of the experiments on cesium at Laboratoire Aimé Cotton, the hot Rydberg atoms were removed using one of two methods. By

switching off the trap and repump laser beams 50–100 ns before the arrival of the dye laser pulse, most of the hot $6p_{3/2}$ atoms were lost, while there was still a significant cold $6p_{3/2}$ population due to radiation trapping. Alternatively, the trap and repump laser beams were switched off 20 μs before the dye laser pulse. This time is sufficient for most of the hot and cold Cs atoms to decay to the $6s_{1/2}$ state. Cold Cs atoms were then pumped back to the $6p_{3/2}$ state using a weak laser diode beam copropagating with the dye laser beam and resonant with the Cs $6s_{1/2}$ $F=4 \rightarrow 6p_{3/2}$ $F=4$ transition. Note that this laser is exactly resonant, and not red detuned like the trap lasers. This resonant laser is turned on 500 ns before the dye laser pulse arrives. While all the cold atoms can be excited by the resonant diode laser, only the hot atoms with velocities perpendicular to the laser propagation direction can be, with the result that the hot Rydberg population is suppressed by 98% [14]. We were careful to minimize the effects of amplified spontaneous emission (ASE) from the dye laser in our experiments. ASE is capable of causing photoionization, possibly providing the initial ionization required to trap the electrons liberated. We minimized ASE either by careful alignment of the dye lasers, or using a diffraction grating and spatial filter to remove the continuum background before the pulse entered the MOT apparatus. Estimates of absolute Rydberg atom population densities are uncertain by a factor of 3, though relative populations can be measured to 10%.

Excitation of the Rydberg atoms takes place at the symmetry point of an electrode geometry that is used to apply electric fields to the Rydberg atoms. The main field that we apply is a positive- or negative-polarity pulse of up to several kV/cm and a rise time of 1 μs that is used to field-ionize the Rydberg atoms and push the resulting positive ions or electrons towards a microchannel plate (MCP) detector. This pulse is applied at a variable time interval after the dye laser pulse, thus allowing the Rydberg-plasma evolution for a time interval that is controllable from 100 ns up to 1 ms. The lower limit of this time interval is set by electrical noise and photoelectron contamination from sources having nothing to do with the trapped atoms, while the upper limit is the maximum time at which we could practically observe a signal. (It should be noted that we were able to see the plasma persist for ~80 μs, much longer than the 30 μs that was observed in the initial studies [14,18].) The electric field pulse also pushes free electrons or ions from the plasma into the MCP, and the plasma signals are temporally separated from the field ionization signals. In addition, the electrodes are used to apply dc electric fields, to observe the effect of quenching the plasma, and also to apply rf fields to heat the plasma electrons. During the course of the experiments described here, two different electrode geometries were used. First, a pair of optically transparent conducting meshes were used to apply the electric fields. Second, in our later experiments, the electric fields were applied using a four-wire geometry. This difference had no material effect on the phenomena being investigated.

To determine the time dependence of the evolution of the Rydberg atoms into a plasma, we first simply varied the time at which we applied the field ionization pulse. This straightforward approach failed because of the large shot-to-shot variation in the number of Rydberg atoms produced and the
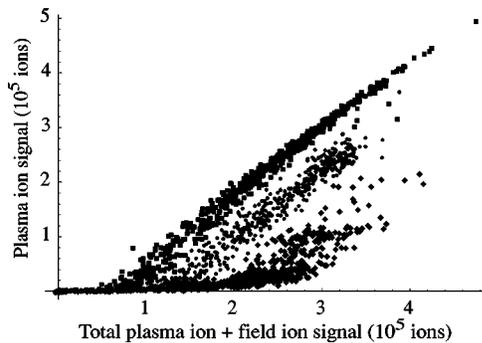
FIG. 1. Binned data showing the dependence of plasma ion number on the total detected ion signal (plasma ions + field ions) for Rb 36d at delays of 2 μs ($\blacklozenge$), 5 μs ($\bullet$), and 12 μs ($\blacksquare$) from the laser pulse.

inherently nonlinear character of the formation of the plasmas. The shot-to-shot variation comes from the mode structure of the dye laser.

Within the dye laser linewidth of 0.3 cm^{-1} (9 GHz), there are roughly 15 cavity modes 750 MHz apart, and which ones oscillate on any given shot of the laser is random. Since the linewidth of the transition from the Rb $5p_{1/2}$ or Cs $6p_{3/2}$ state to a Rydberg state is only 5 MHz, the randomness of which modes oscillate leads to enormous shot-to-shot fluctuations in the number of Rydberg atoms produced. To make quantitative measurements of the time dependence of the evolution to a plasma, we used a binning approach. Specifically, we fixed the time delay of the ionization pulse and set gated integrators on the signals from the plasma ions and the field ionized atoms and recorded both signals on every shot of the laser. We then binned the data according to the sum of the two detected ion signals, which was assumed to reflect the initial Rydberg population. The shot-to-shot fluctuations of the laser in combination with neutral density filters allowed us to generate plots such as the one shown in Fig. 1, which is for the Rb 36d state at delays of 2, 5, and 12 μs. Data were collected at 100 ns intervals in the delay time. By taking slices, i.e., at the same number of initial Rydberg atoms, through the data we could construct the time dependence of the evolution to a plasma. The obvious kinks in the data at 0.8×10^5, 1.2×10^5, and 2.0×10^5 correspond to the points to the points at which enough ions had accumulated to trap any electrons subsequently liberated.

III. INITIAL IONIZATION MECHANISMS

In the original experiments, the initial ionization was attributed to photoionization by blackbody radiation and collisions between Rydberg atoms. For states of $n < 40$, the plasma only formed when hot (300 K) atoms were present, but for $n > 50$ the plasma formed in the absence of hot atoms as well. To separate these effects, we have examined the n dependence of the initial ionization mechanism. In particular, we have measured the threshold number of Rydberg atoms needed to initiate the avalanche ionization, N_T, as a function of n. Specifically, we have made measurements for the Cs 26d to 55d states using mixtures of hot and cold atoms with
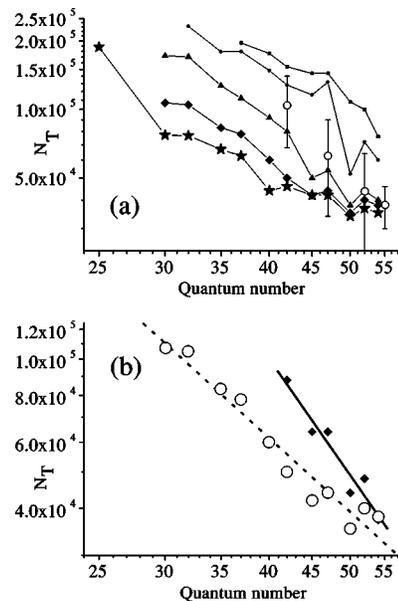

FIG. 2. (a) Log-log plots of the threshold number of Rydberg atoms, N_T, needed to initiate avalanche ionization for Cs states from 26d through 55d and 48s through 59s, in a sample with approximately 1% of 300 K Rydberg atoms. These data were obtained at delays between the laser and beginning of the field pulse of 1 μs ($\blacksquare$), 2 μs ($\bullet$), 5 μs ($\bullet$), 10 μs ($\blacklozenge$), and 20 μs ($\star$) for nd states, and 5 μs ($\circ$) for ns states. (b) Log-log plots of N_T versus n at a delay of 10 μs for purely cold Rydberg samples ($\blacklozenge$), and for mixed samples containing approximately 1% of thermal Rydberg atoms ($\circ$). As can be seen, the threshold Rydberg atom numbers are approximately a factor of 2 higher for a purely cold sample. Also shown are fits of N_T versus n, which shows $N_T \propto n^{-3.2}$ for a purely cold sample (—) and $N_T \propto n^{-2.1}$ for a mixed sample (---).

delay times of 2–20 μs. In addition, we have observed ns states of cesium from 48s to 59s to spontaneously evolve to plasma, a phenomenon that was not observed in the initial experiments [14]. We include both the ns (for a delay time of 5 μs only) and nd data in Fig. 2(a). We have also taken data analogous to those shown in Fig. 2(a) for purely cold samples of atoms for the Cs 30d to 54d states. As shown by Fig. 2(a), N_T decreases rapidly with n in a manner that is independent of the interaction time. To display this phenomenon quantitatively, we show log-log plots of N_T versus n in Fig. 2(b), which contains the data for both hot-cold mixtures and purely cold samples. Both data sets were obtained using a delay of 10 μs between the laser and field ionization pulse.

From Fig. 2(b), it is apparent that $N_T \propto n^{-2.1}$ for the hot-cold mixtures, while for a purely cold sample, $N_T \propto n^{-3.2}$, and that for high n, N_T is roughly a factor of 2 higher for purely cold atoms than for mixtures containing $\sim 1\%$ hot atoms. We can compare the experimental observations of Fig. 2(b) to the expected results for initial ionization due to blackbody radiation and collisions. First, we consider the expected dependence due to blackbody ionization. The average excess kinetic energy of the blackbody photoelectrons is $\Delta \overline{E} = \overline{E}_\gamma - E_R$, where $E_R = 2R/2n^{*2}$ is the modulus of the Rydberg energy (where R is the Rydberg constant in units of energy) and $\overline{E}_\gamma$ is the average blackbody photon energy absorbed by a Rydberg atom during the ionization process. These electrons

will be trapped when their kinetic energy ΔE is equal to the magnitude of the trapping potential U_i of the macroscopic positive ion cloud. Following Killian *et al.*, we assume a spherically symmetric ion sample where N_i positive ions have a Gaussian density distribution of characteristic radius r [7]. The potential binding energy has a maximum magnitude U_i, where

$$U_i = \sqrt{\frac{2}{\pi}} \frac{N_i e^2}{4\pi\epsilon_0 r}. \qquad (1)$$

Setting $\Delta E = U_i$ and assuming that the N_i positive ions are produced by photoionization of N_T initial Rydberg atoms during the initial ionization phase of duration t_{int}, we can calculate the threshold number of Rydberg atoms required. We set $N_i = N_T t_{int} \Gamma_b$, where Γ_b is the blackbody photoionization rate,

$$\Gamma_b \propto \int_{E_R}^{\infty} \sigma_{E_R}(E_\gamma) \frac{E_\gamma^2}{e^{E_\gamma/k_B T} - 1} - dE_\gamma, \qquad (2)$$

where $\sigma_{E_R}(E_\gamma) \propto E_\gamma (E_R^{3/4} E_\gamma^{-5/3})^2$ is the photoabsorption cross section of a Rydberg state with energy $-E_R$ for photons of energy E_γ [19,20]. Similarly, $\bar{E}_\gamma$ may be calculated using

$$\bar{E}_\gamma = \frac{\displaystyle\int_{E_R}^{\infty} E_\gamma \sigma_{E_R}(E_\gamma) \frac{E_\gamma^2}{e^{E_\gamma/(k_B T)} - 1} dE_\gamma}{\displaystyle\int_{E_R}^{\infty} \sigma_{E_R}(E_\gamma) \frac{E_\gamma^2}{e^{E_\gamma/(k_B T)} - 1} dE_\gamma}. \qquad (3)$$

Evaluating Eqs. (2) and (3) numerically, and then finding $\Delta\bar{E}$, we find that, for $25 < n^* < 40$ and $T = 300$ K, $\Delta E \approx (n^*/25)^{-0.56}(k_B \times 225\text{K})$ and $\Gamma_b \propto (n^*)^{-0.8}$. Assuming that the physical extent of the Rydberg sample remains roughly constant, and using the formulas above to relate $\bar{E}_\gamma$ and Γ_b to N_T, we find that N_T is roughly proportional to $(n^*)^{1/4}$ for $25 < n^* < 40$. This strongly disagrees with the experimental data, which fit an $(n^*)^{-2.1}$ law. In other words, while there is good evidence to suggest that blackbody ionization contributes to the preavalanche process (we discuss further evidence below), it is apparent from the n dependence of Fig. 2 that it is not the major source of the initial ionization.

While blackbody photoionization rates decrease with n, the collisional ionization cross sections increase, presumably as the geometric cross sections, $\sigma_g = \pi(a_0 n^2)^2$, and, as we shall show, such a dependence is more likely to lead to the n dependence of N_T shown in Fig. 2(b). In most of our experiments, there are of order 1% hot Rydberg atoms, excited from the background vapor, and it is instructive to calculate the expected value of N_T which would result from hot-cold Rydberg ionizing collisions. The hot-cold Rydberg ionization collision cross section is of order $\sigma_g = \pi(a_0 n^2)^2$, the geometric cross section. If one uses an effective cross section of $A\sigma_g$, where A is expected to be of order 10 [16,21], the collisional ionization rate for hot atoms in Rydberg-Rydberg collisions is $\Gamma_c = ANv_{rel}\sigma_g / \pi l \omega_o^2$, where l and ω_o are the length and radius of the pulsed laser interaction region with the atoms, respectively, N is the number of Rydberg atoms, and v_{rel} is the relative velocity of colliding atom pairs. The

number of ions, N_i, that are created by collisions in a time t_{int} from N Rydberg atoms during the slow preavalanche process is $N_i = BN t_{int} \Gamma_c$, assuming that these collisions are the only process that contributes to ionization during this time. The numerical factor $B \approx 0.01$ accounts for the fact that 1% of the atoms are hot. N_i can be related to the resulting potential well depth of the positive ions using Eq. (1). We make the somewhat simplistic assumption that when $N = N_T$, $U_i = \Delta E = E_R = 2R/2n^2$, i.e., that the threshold to avalanche occurs when the Rydberg atom number is such that the resulting ions create a positive potential well that traps electrons of kinetic energy equal to the binding energy of the initial Rydberg state. Hence, we obtain

$$\frac{2R}{2n^2} = \sqrt{\frac{2}{\pi}} \frac{e^2}{4\pi\epsilon_0 r} \frac{ABv_{rel} a_0^2}{l\omega_o^2} t_{int} \, n^4 \, N_T^2, \qquad (4)$$

and hence that $N_T \propto n^{-3}$. This model is clearly oversimplified. We assume that the threshold condition is given by $\Delta E = 2R/2n^2$, and that the plasma has a spherical geometry while the Rydberg sample from which it derives is cylindrical. We do not consider the distribution of collision velocities, or any effect of Rydberg redistribution. Finally, we assume that the contribution of blackbody radiation is negligible. Nevertheless, the predicted dependence of N_T on n is very close to the $n^{-2.1}$ dependence shown by the data in Fig. 2, and we therefore feel that the Rydberg-Rydberg collision process is significant in the preavalanche regime. The comparison between the simple model presented above and the data of Fig. 2 suggests that when hot atoms are present, hot-cold, Rydberg-Rydberg collisional ionization is the dominant initial ionization mechanism. However, when there are no hot Rydberg atoms, a plasma still forms for high n states. This phenomenon has been observed in our experiments and those in which Rb np states are excited from the ground state, with no $5p$ atoms present [2]. Measurements of N_T for purely cold atoms of $n > 40$, shown in Fig. 2(b), show an $n^{-3.2}$ dependence similar to that seen for hot-cold mixtures, although the required values of N_T are higher. Nonetheless, the results are consistent with a collision process with an n^4 scaling of the cross section. Although there are as yet no data which unambiguously identify the mechanism, several possibilities consistent with the observations of Fig. 2(b) present themselves. First, it may be that the ionization comes from static overlap or slow collisions between pairs of closely spaced Rydberg atoms. Second, resonant dipole-dipole energy transfer has already been observed in cold Rydberg gases, and it has been suggested that one atom could be ionized while the other goes to lower energy, although much higher densities than used here should be required. However, a sequence of dipole-dipole energy transfers might lead to the observed result at the densities of our experiments. Finally, long-range forces, (induced) dipole-charge or dipole-dipole, can attract Rydberg atoms leading to efficient autoionizing Rydberg-atom pairs [22]. This mechanism was suggested to explain the avalanche ionization of dense thermal samples of Cs Rydberg atoms reported by Vitrant *et al.* [16].

As demonstrated by Vitrant *et al.*, hot 300 K Rydberg atoms evolve into a plasma if they are dense enough,
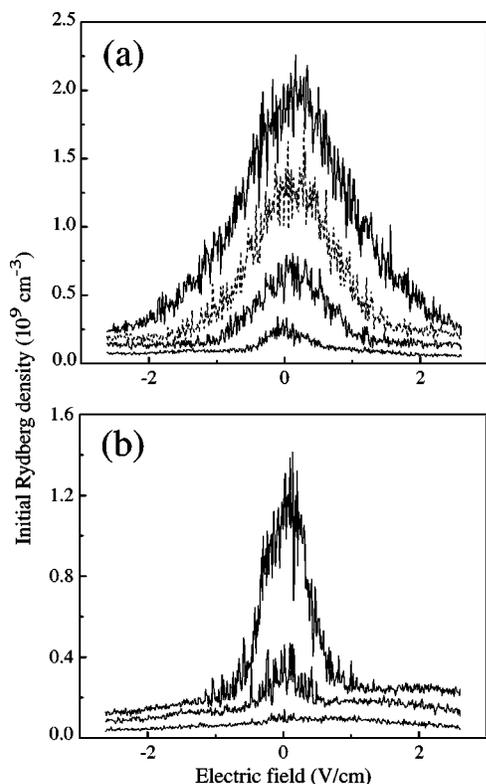
FIG. 3. Electric field dependence of the plasma ion signal for two different Rydberg states, 41d (a) and 32d (b). Each graph plots several different initial Rydberg population densities, which are, from top to bottom in each of (a) and (b), 2.5×10^9 cm^{-3}, 1.5×10^9 cm^{-3}, 1.0×10^9 cm^{-3}, and (for 41d only) 0.4×10^9 cm^{-3}. The data were obtained at a delay of 10 μs from the laser pulse, and each data point is averaged over 30 laser shots.

$\sim 10^{11} - 10^{12}$ cm^{-3} for $n=30-45$. However, to form a plasma from $n=30$ Rydberg atoms at a density of 10^9 cm^{-3}, the atoms must be cold. We demonstrated this point by exciting similar numbers of hot and cold Rb 40d atoms. Using only hot atoms, no plasma forms [14]. A slightly different way of seeing the importance of having cold atoms is to apply a static field and observe the plasma signal versus field. The plasma (ion) signals observed after 10 μs for initial Rb 32d and 41d atoms are shown in Fig. 3. The result is exactly opposite what one would naively expect for Rydberg states. It takes more field to suppress the formation of the plasma for the 41d state than for the 32d state. The reason that plasma formation from the 32d state can be suppressed by smaller fields is that the initial ionization of the 32d state is slower and the macroscopic ion cloud which binds the plasma electrons is formed over a longer period of time. In 1 μs, a ^{85}Rb$^+$ ion initially at rest in a 1 V/cm field moves 55 μm, half the trap radius. Consequently, in the several microseconds required to accumulate enough ions from the Rb 32d state, the ions are dispersed over distance larger than the original trap radius.

IV. ACCELERATION OF THE AVALANCHE IONIZATION BY ADDING ENERGY

The most puzzling aspect of our initial experiments was that it appeared that all the Rydberg atoms were converted to

the plasma. In the plasma, the electrons are essentially free, while in the Rydberg atoms they are bound by ~ 100 cm^{-1} ($n=30$), so the conversion of all the Rydberg atoms to the plasma appears to violate the principle of conservation of energy.

As a direct test of whether or not adding energy accelerates the formation of the plasma, we have investigated the effect of heating the free electrons using radiofrequency (rf) fields. The weak rf fields (~ 1 V/cm at 100 MHz) should cause negligible perturbation of the Rydberg atoms, but the free electrons will oscillate, thereby gaining a time-varying kinetic energy. Hence, the rf field should have no effect on the initial slow ionization process, since it is caused by blackbody radiation and hot Rydberg–cold Rydberg collisions, and electrons are not involved. On the other hand, the avalanche ionization process may be significantly enhanced. (In the experiments on cold plasmas by Kulin *et al.* [6], rf fields were used to resonantly drive the collective plasma oscillation frequency, which in their work had a maximum frequency of 250 MHz, corresponding to an electron density of 8×10^8 cm^{-3}. In our experiments, we used frequencies from 70 to 300 MHz, corresponding to the plasma frequencies for electron densities from 2.2×10^8 to 1.0×10^9 cm^{-3}. During the avalanche ionization, the electron density rises from zero to a density corresponding to a plasma frequency in excess of our rf frequencies. In these experiments, we were only able to detect ions. Had we been able to detect electrons, it might have been possible to discriminate between depositing energy into the plasma and into individual electrons. At the onset of the avalanche, the electron density is low, and it is reasonable to treat the electrons as free electrons interacting with the rf field.)

Averaged over one cycle of the rf field, the energy of an electron in the rf field is just the well-known ponderomotive energy, given in atomic units by

$$E_p = \frac{F^2}{4\omega^2}, \tag{5}$$

where F is the amplitude of the rf field and ω is its angular frequency (both expressed in atomic units). For $\omega/2\pi$ corresponding to 100 MHz, $F=1$ V/cm and $E_p=9$ cm^{-1}. The rf field has two effects on the plasma evolution process. First, it increases the electron-Rydberg collision rate, since the free electron is moving faster. Second, the amount of energy that the free electron can transfer to the Rydberg electron is increased, since the energy of the free electron has increased, on average, by the ponderomotive energy. However, considering the average energy gain of the free electron does not reveal the whole story, since the maximum energy that the free electron may have in the field is much greater than E_p. For an electron with initial kinetic energy K_i, the maximum energy that can be gained from the rf field is

$$E_{\max} = \sqrt{8 K_i E_p} + 2 E_p, \tag{6}$$

which, for the example previously cited with an electron that has $K_i=20$ cm^{-1}, corresponds to an energy gain from the rf field of 56 cm^{-1}, or a total energy of 76 cm^{-1}. This energy is comparable to the binding energy of the Rb 39d state. We
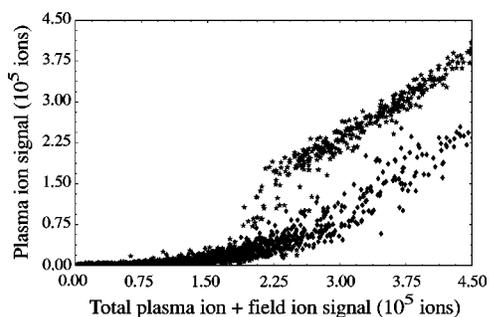
FIG. 4. Binned data at a delay of 10 μs for Rb showing the effect of rf fields on the spontaneous plasma formation process. Data taken with no rf present are denoted by $\blacklozenge$, while data taken with a 100 MHz, 0.5 V/cm field are shown thus: $\bigstar$. The data are plotted vs the total detected ion signal (plasma ions + field ions) on the x axis, which is assumed to be equal to the initial Rydberg population.

have carried out experiments at fixed time delay between the laser and field ionization pulse, where the data are binned as described above, in the presence of rf fields. The rf field has a rise time of 0.5 μs, and is turned on immediately after the laser pulse excites the Rydberg state. The rf field remains on until after the field ionization pulse is turned off.

Data obtained by binning the plasma signal at a fixed delay of 10 μs both with and without the 100 MHz rf field may be seen in Fig. 4, obtained with the Rb $32d$ state initially populated by the laser. As can be seen, the presence of the rf gives a much more distinct threshold for the onset of the avalanche at a total ion signal of approximately 2×10^5 ions, corresponding to a Rydberg atom density of 5×10^9 cm^{-3}. We have observed analogous effects due to the rf for the $32d$, $38d$, and $42d$ states. These data clearly demonstrate that adding energy speeds up the evolution to a plasma.

Finally, we investigated the behavior of the plasma evolution process as a function of rf frequency and amplitude. These data were obtained as a function of delay between the laser and field ionization pulse, for total number densities of Rydberg atoms in the range $(4$–$6) \times 10^9$ cm^{-3}. At a fixed amplitude of 0.94 V/cm, $40d$ Rydberg atoms evolved to plasma once the avalanche regime was reached more rapidly when the rf frequency was 70 MHz than when it was 100 MHz, and that rate was higher at both these frequencies than when no rf was present. However, there was no meaningful enhancement of the ionization when the rf frequency was 300 MHz. These findings basically confirm that avalanche ionization rates are higher when the free electron ponderomotive energy is increased, as expected. At 100 MHz, when the rf amplitude is increased from 0.94 V/cm to 2.62 V/cm, however, the avalanche process occurs at a lower rate than with no rf present, since the maximum distance that the electron moves per cycle is 115 μm, so free electrons tend to leave the interaction region before they can enhance the avalanche ionization process. On the other hand, increasing the amplitude to 3.0 V/cm at 300 MHz increases the avalanche ionization rate for the $35d$ state compared to the rate at 0.94 V/cm, since at 3.0 V/cm and 300 MHz, the maximum electron displacement per cycle is 15 μm, much less than the
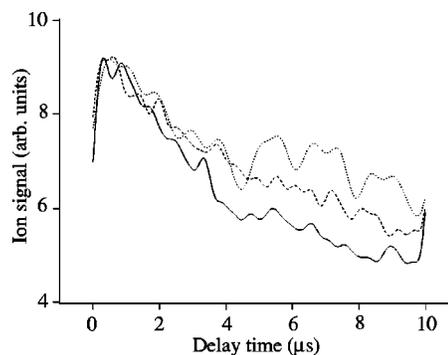

FIG. 5. Averaged positive ion signals (plasma ions plus field ions) from the Rb $44d$ state as a function of delay for different field pulse maximum amplitudes: 310 V/cm (—), 620 V/cm (- - -), and 1500 V/cm (···). The adiabatic threshold for ionization of the Rb $44d$ state is 97 V/cm, and zero on the y axis corresponds to the signal when the dye laser is blocked.

sample size, while the ponderomotive energy is now comparable to that in a 100 MHz field of amplitude 1 V/cm.

V. RYDBERG POPULATION REDISTRIBUTION

The rf heating experiments described in the preceding section demonstrate that forming the plasma is accelerated by adding energy, irrespective of whether the rf field deposits energy in free electrons or the plasma. We now return to the question of the source of that energy in the absence of rf heating. Our recent experiments show that population is transferred from the initially excited Rydberg state to lower-lying states. In particular, we have made observations using ion and electron detection. The ion signal represents the sum of the number of ions in the plasma and those generated by field ionization of Rydberg atoms.

We observed the total ion signal (plasma ions and field ions) by setting the gate of a boxcar averager so that it included both signals. This signal was obtained in rubidium for two initial states, $44d$ and $36d$, as a function of delay between the laser pulse and field ionization pulse in the range 0–10 μs (care was taken to subtract off the background by taking duplicate data sets with the dye laser pulse blocked). For the $44d$ states, we obtained these data for three different amplitudes of field ionization pulse. Specifically, the field ionization pulse amplitudes were set to maximum values of 310 V/cm, 620 V/cm, and 1500 V/cm, values which are, respectively, 3.2, 6.4, and 15.4 times the adiabatic threshold for ionization of the Rb $44d$ state (97 V/cm). The smallest field pulse amplitude was chosen so that it approximately corresponds to the nonadiabatic ionization threshold for n^* $=44$. In other words, we can be reasonably sure that a pulse of amplitude 310 V/cm will ionize all ℓ-states for $n^* \geqslant 44$, and at least some ℓ-states as low as $n^*=32$, but this pulse cannot ionize any states that have $n^* < 32$. In Fig. 5, we show the total ion signal obtained with an initial Rb $44d$ density of 4.0×10^9 cm^{-3} and peak ionization fields of 310, 620, and 1500 V/cm. The data shown in Fig. 5 show loss of signal as a function of delay that depends on the amplitude of the field ionization pulse. This loss of signal is clearly caused by

mechanisms other than radiative decay, since the radiative lifetime of the Rb 44d state is in excess of 70 μs [23]. The rate of depopulation of the 44d state due to blackbody stimulated transitions corresponds to an effective lifetime of 88 μs [24], and the strongest transitions are to nearby states that will field ionize in the pulse that we apply. Hence, we can be sure that the decline in the ion signal as a function of delay is due to collisional processes that drive population to states that cannot be field ionized in our pulse. This hypothesis is supported by the fact that as the pulse amplitude is increased from 310 V/cm to 620 V/cm and 1500 V/cm, we can see that the loss of signal as a function of delay becomes progressively less, but there is some loss of signal even at 1500 V/cm, a field that will adiabatically ionize states as low as $n^* = 21.5$. The data shown in Fig. 5 thus support the theoretical finding reported in a paper by Robicheaux and Hanson [9] that free electrons are heated by collisions with high-ℓ states of the same n as that initially populated by the laser, which results in conversion of these states to those of lower n which are harder to field ionize. We point out, however, that the maximum loss of signal in the first 10 μs for 44d even with a pulse of 310 V/cm, 3.2 times the adiabatic limit for this state, is only 40% or so. Therefore, these data in no way invalidate our practice of binning in some experiments, as described above. This is because the signal fluctuations that are due to laser pulse frequency shifts and shot-to-shot energy variation have a much greater impact on the binned signal than the relatively small effect caused by Rydberg population migration to lower n states.

The decrease of the signals shown in Fig. 5 with time is due to superelastic collisions of plasma electrons with 44d Rydberg atoms. These collisions drive the atoms to states too low in energy to be detected by field ionization. Since the plasma electrons are generated by processes nonlinear in the number of Rydberg atoms, the relatively rapid time decays shown in Fig. 5 should only occur at high densities of Rydberg atoms. In fact, this appears to be the case as shown by Fig. 6, which shows the loss of signal when the Rb 44d state is initially populated by the laser. The signal is from plasma ions and Rydberg states that field ionize in a field that is 3.2 times the adiabatic limit for 44d. In Fig. 6, the four traces correspond to different dye laser pulse energies and hence different initial Rydberg densities (the laser was attenuated using neutral density filters). The rate of population loss due to migration to more deeply bound states is significantly higher at high Rydberg densities than at lower densities.

One of the puzzling aspects of our initial experiment was that there was no clear indication of population in any bound state other than the one excited by the laser. As shown by the measurements described in the previous section, there is clear evidence that when high densities of Rydberg atoms are excited, there is population transfer to states which lie too low in energy to be field ionized. To obtain a better idea of the distributions of states which are populated, we have used electron detection in conjunction with field ionization. The flight time of the electrons to the detector is negligible compared to the rise time of the field pulse, so the time at which the electron signal is detected tells us immediately the field at which the atom was ionized. The predominant scattering process in the formation of the plasma is electron scattering
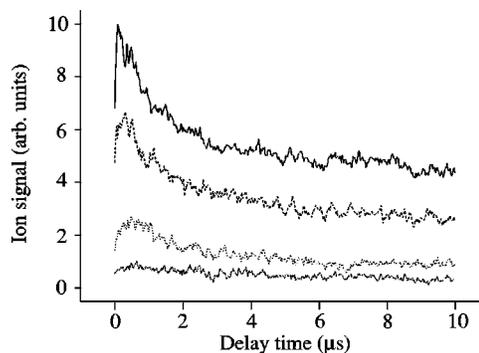

FIG. 6. Averaged positive ion signals (plasma ions plus field ions) from the Rb 44d state as a function of delay for different initial Rydberg atom densities. These data were obtained with field ionization pulse amplitudes of 310 V/cm, a value that is 3.2 times the adiabatic ionization threshold for 44d. Zero on the y axis corresponds to the signal when the dye laser is blocked. Each data trace was obtained by placing different neutral density filters in the dye laser beam. The average Rydberg atom densities are (from top to bottom) 4.0×10^9 cm^{-3}, 1.3×10^9 cm^{-3}, 7.2×10^8 cm^{-3}, and 4.0×10^8 cm^{-3}.

from Rydberg atoms. Initially one would expect ℓ-mixing collisions, followed by n-changing and ionizing collisions. Ionizing collisions are simply the continuation of n-changing collisions across the limit, so a reasonable expectation is that we would find n states both above and below the state initially populated.

In Fig. 7, we show the field ionization traces obtained using the Rb 44d state with a delay of 100 ns for the ionization pulse, which has amplitude 1500 V/cm. With no neutral density filter in the laser, the initial Rydberg-atom population is 4.0×10^9 cm^{-3}. In Fig. 7(a), we show the signal obtained a ND 2.5 filter in the laser. The signal observed at this low density is from primarily adiabatic ionization of the 44d state. With a ND 1.5 filter, we observe the trace of Fig. 7(b), in which there is now an obvious later field ionization component, with a peak at 0.93 μs and extending to 1.3 μs. We attribute it to diabatic ionization of $n=44$ states of higher ℓ and m. (In most of the traces of Figs. 7 and 8 there are artifacts due to ions which have hit electrodes and generated secondary electrons. They are most prominent at 3.0 and 3.5 μs, but also occur at 2.5 μs in traces in which there is a large plasma signal.) Figure 7(c) shows the result observed with a ND 1.0 filter. Two new features are now apparent. First, a small plasma signal is now evident at t$=0.50$ μs. Second, it is now clear that the ionization signal extends to longer times, reflecting population transfer to lower-lying states. In Fig. 7(d), taken at 100 ns with an ND 0.5 filter, several features are clear. There is more plasma signal, at $t=0.5$ μs, and a continuous Rydberg signal from the plasma signal at 0.5 μs to 0.9 μs, signifying the population of higher-lying, $n>44$, states. Finally, there is now an evident tail of the signal extending to very long times, which correspond to higher ionization fields and lower-lying states. Figure 7(e) shows the result with a delay of 100 ns and no ND filter. Under these conditions, the plasma signal extends from $t=0.5$ to 0.9 μs with a peak at 0.7 μs, and it evidently overlaps the signal from field ionization of the $n=44$ states. At
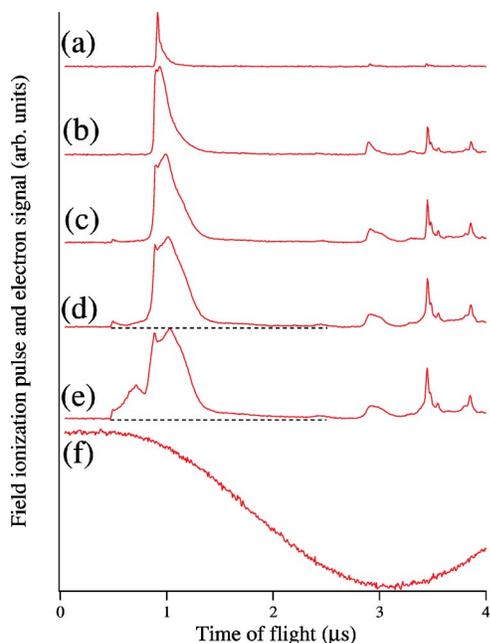
FIG. 7. Averaged electron field ionization signals from the $44d$ state at a delay of 100 ns between the laser pulse and the beginning of the field ionization pulse, obtained with a maximum field of 1500 V/cm. Data were obtained with different initial Rydberg atom densities using neutral density filters placed in the pulsed laser beam. The atom densities relative to that when the laser was unattenuated are given by 10^{-D}, where D is the filter density. We show data for (a) $D=2.5 \Rightarrow 1.3 \times 10^7$ cm^{-3}, (b) $D=1.5 \Rightarrow 1.3 \times 10^8$ cm^{-3}, (c) $D=1.0 \Rightarrow 4.0 \times 10^8$ cm^{-3}, (d) $D=0.5 \Rightarrow 1.3 \times 10^9$ cm^{-3}, and (e) no ND filter, $D=0 \Rightarrow 4.0 \times 10^9$ cm^{-3}. We also show the field ionization pulse (f), which has a maximum amplitude of 1500 V/cm. The horizontal dashed lines in (d) and (e) show the zero level of the electron signal.

this point, when the plasma has a small radius but contains many ions, a substantial field is required to remove the last electrons from the plasma. In Fig. 7(f), we show the field ionization pulse.

In Fig. 8, we show the field ionization signals obtained when exciting the Rb $44d$ state and applying the same 1500 V/cm field pulse used to obtain the data of Fig. 7. In all cases but one, the initial Rydberg-atom population is 4.0×10^9 cm^{-3}. For reference, in Fig. 8(a) we show the signals obtained with a 100 ns delay with a ND 2.5 filter and without a filter. [These are also shown in Figs. 7(a) and 7(e), respectively.] In Fig. 8(b), we show the signal obtained with a 1 μs delay time. At this point, the adiabatic $n=44$ signal has almost disappeared into the plasma signal, and there is now a very pronounced long time (high field) tail to the signal. Figure 8(c) shows the data obtained with a 5 μs delay, when most of the atoms have been ionized and the plasma has expanded so that it has become easier to liberate electrons from the field of the positive plasma ions. At a delay of 30 μs [Fig. 8(d)] the plasma signal has almost disappeared and is quite narrow since the plasma has expanded to the point that, even with many ions present, the last electrons to be extracted are weakly bound. There is no trace of the original $44d$ state. Instead, only more deeply bound states, ioniz-
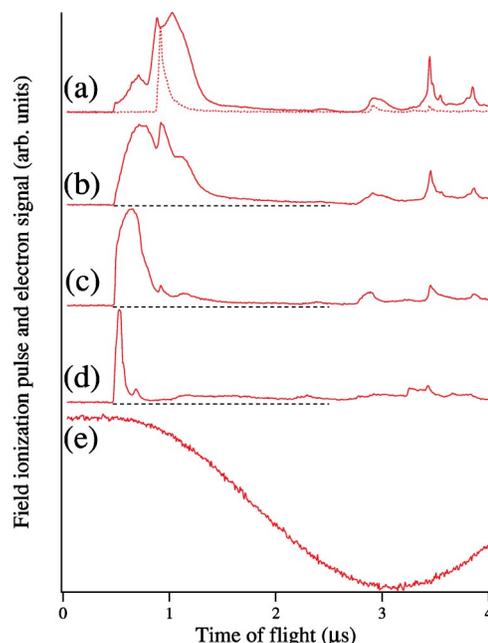

FIG. 8. Averaged electron field ionization signals from the $44d$ state at various delays between the laser pulse and the beginning of the field ionization pulse, obtained with a maximum field of 1500 V/cm and a density of 4.0×10^9 cm^{-3} [except for the dotted line in (a)]. Data were obtained at delays of (a) 100 ns, for which data are shown with the dye laser pulse unattenuated (solid line), and attenuated with a $D=2.5$ filter to a density of 1.3×10^7 cm^{-3} (dotted line), (b) 1 μs, (c) 5 μs, and (d) 30 μs. The horizontal dashed lines in (b), (c), and (d) show the zero level of the electron signal.

ing at fields from 200 V/cm to 1400 V/cm, are observed. In sum, the data shown in Figs. 7 and 8 confirm many aspects of the scenario outlined by Robicheaux and Hanson. However, one feature they do not demonstrate very well is that ionizing electron-Rydberg collisions are simply the extension of n-changing collisions across the ionization limit. To demonstrate this point more clearly, we have recorded the field ionization signals with a lower amplitude pulse.

In Fig. 9, we show the field ionization signal from atoms initially excited to the Rb $44d$ state obtained with a pulse of 105 V/cm amplitude. With the full dye laser power, we produced an initial Rydberg-atom population of 4.0×10^9 cm^{-3}. With a ND 2.0 filter and a 100 ns delay, we observe the signal shown in Fig. 9(a). It corresponds to the essentially adiabatic ionization of the Rb $44d$ state. Using a ND 1.5 filter and a 100 ns delay, we observe the trace of Fig. 9(b), in which a nonzero signal extends from $t=800$ ns to the $44d$ signal at 3 μs. This signal demonstrates that all n states between $n=44$ and the limit are populated, as might be expected from the continuity of the ionization cross section at the ionization limit. As shown by Fig. 9(c), when a ND 1.0 filter is used, there is more transfer to high n states, and a plasma forms, leading to the broad peak at 1.4 μs, which overlaps the adiabatic Rydberg signal for $n>60$. The plasma signal does not appear at the onset of the field ionization pulse but later due to the difficulty in extracting the electrons from the large number of positive ions present. As shown by Fig. 9(d), with no ND filter and a 100 ns delay the plasma
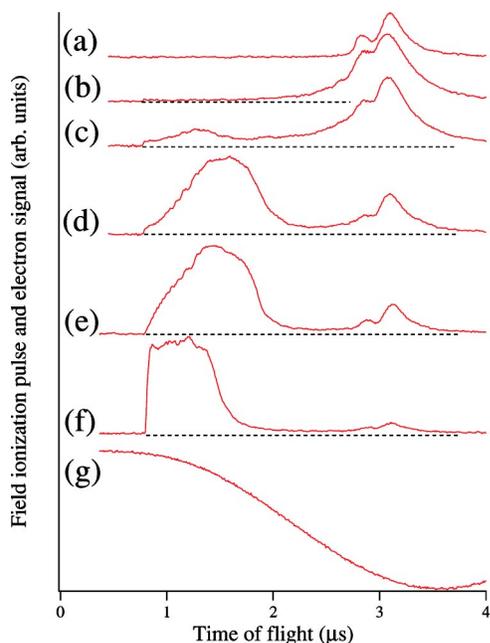
FIG. 9. Averaged electron field ionization signals from the $44d$ state at various delays between the laser pulse and the beginning of the field ionization pulse and various initial Rydberg-atom number densities, obtained with a maximum field of 105 V/cm. We show data for (a) a delay of 100 ns and $D = 2.0 \Rightarrow 4.0 \times 10^7$ cm^{-3}, (b) a 100 ns delay and $D = 1.5 \Rightarrow 1.3 \times 10^8$ cm^{-3}, (c) a delay of 100 ns and $D = 1.0 \Rightarrow 4.0 \times 10^8$ cm^{-3}, (d) a delay of 100 ns and no ND filter $\Rightarrow 4.0 \times 10^9$ cm^{-3}, (e) a delay of 1 μs and no ND filter, and (f) a delay of 5 μs and no ND filter. For reference, we also show the field ionization pulse (g), which has a maximum amplitude of 105 V/cm. The horizontal dashed lines show the zero levels of the electron signal.

signal is much larger, and it now requires a much larger field to extract all the electrons from the plasma, as can be expected from the much higher number of ions in the plasma. As shown in Fig. 9(e), at a delay of 1 μs it becomes easier to remove the first half of the electrons from the plasma, although the last ones are still as hard to remove as at 100 ns, because the plasma has not yet expanded substantially. Relative to the 100 ns trace of Fig. 9(d), the number of bound Rydberg atoms has decreased. As shown by Fig. 9(f), by 5 μs it is evident that the plasma has now expanded since it is now easier to remove the last of the plasma electrons due to expansion of the ion cloud. To be a little more precise, the field required to remove the last plasma electrons in Fig. 9(f) is half the field required to remove the last plasma electrons in Fig. 9(e). The number of ions is the same, so the radius of the plasma has presumably doubled, which is consistent with the 40 m/s plasma expansion velocity observed by Kulin *et al.* [6]. For reference, we show in Fig. 9(g) the field ionization pulse.

Our results from the electron time-of-flight spectra are in good general agreement with those reported in a recent paper by a group at the University of Michigan. Specifically, Walz-Flannigan *et al.* [17] used a 100 μK sample of Rydberg rubidium atoms at a maximum density of $\approx 1 \times 10^9$ cm^{-3}. They found evidence for ℓ mixing caused by electron–Rydberg-

atom collisions with a signature that is basically identical to that which we observed (e.g., the hump that ionizes in fields between one and four times the adiabatic limit for the initial Rydberg state populated by the laser in Figs. 7 and 8 of this paper). Similarly, they found n-changing electron–Rydberg-atom collisions to states higher in energy than that initially populated, which we also observed, e.g., in Fig. 9 as the "filling-in" in the time-of-flight signal between 2 and 3 μs. Finally, Walz-Flannigan *et al.* also found a significant transfer of population to low-n states (which ionize in fields between four and ten times the adiabatic limit of the initial Rydberg state) at high densities and long delay times. While the theoretical analysis of Robicheaux and Hanson [9] found this phenomenon to be caused by electron collisions with high-ℓ Rydberg states (in other words, the same process that causes high-n population), Walz-Flannigan *et al.* suggest that these states are populated as a by-product of Penning ionization enhanced by dipole-dipole interactions. On the other hand, we observed no signal that persisted for longer than ~ 100 μs after the initial Rydberg state was populated by the laser, whereas an earlier paper from the Michigan group reported seeing electron emission for as long as 20 ms [15]. Some of the differences between our work and that from the University of Michigan are perhaps attributable to the fact that we normally have a small (1–2 %) background of thermal Rydberg atoms, which is completely absent in the Michigan apparatus. Perhaps because of this, similar behaviors are observed at much longer delays after the laser pulse at Michigan than at LAC or UVA. Otherwise, the results of the three experiments are very similar, considering that the work reported in Ref. [17] was confined to initial Rydberg states with $n > 50$ due to a limitation of the magnitude of the field ionization pulse, whereas the UVA and LAC experiments probed down to 26d in cesium.

VI. CONCLUSION

The mechanisms by which dense samples of cold Rydberg atoms spontaneously evolve to plasma have been investigated in a number of different experiments using both rubidium and cesium atoms. We find that the ionization process is initiated by blackbody ionization and Rydberg-Rydberg collisions. However, the ionization rapidly progresses to an avalanche regime at high enough number densities, provided that trapping of free electrons by the charge of positive ions is not inhibited by the application of a static electric field. We find strong evidence for the predictions of a recent theoretical paper [9] that describes the evolution of Rydberg atoms to plasma. Specifically, we find that electron–Rydberg-atom collisions that occur only when there is sufficient positive ion density to trap electrons cause redistribution of population from the initial Rydberg state to nearby high-ℓ states. Subsequent collisions cause both population of lower and higher n states, eventually leading to ionization of a large fraction of the initial Rydberg state atoms, while the remaining population moves to low n states, thereby maintaining the energy balance in the system. Finally, these measurements show that the initial ionization of purely cold Rydberg atom samples occurs by interactions between or among Rydberg atoms.

[1] T. C. Killian, S. Kulin, S. D. Bergeson, L. A. Orozco, C. Orzel, and S. L. Rolston, Phys. Rev. Lett. **83**, 4776 (1999).

[2] D. Tong, S. M. Farooqi, S. Krishnan, J. Stanojevic, Y. P. Zhang, A. S. Estrin, J. R. Ensher, C. H. Cheng, E. E. Eyler, and P. L. Gould, Bull. Am. Phys. Soc. **48**, 101 (2003).

[3] J. R. Guest, J.-H. Choi, A. Povilus, and G. Raithel, Bull. Am. Phys. Soc. **48**, 112 (2003).

[4] N. Vanhaecke, D. Comparat, D. A. Tate, and P. Pillet, e-print quant-ph/0401045.

[5] C. E. Simien, Y. C. Chen, P. Gupta, S. Laha, Y. N. Martinez, , P. G. Mickelson, S. B. Nagel, and T. C. Killian, Phys. Rev. Lett. **92**, 143001 (2004).

[6] S. Kulin, T. C. Killian, S. D. Bergeson, and S. L. Rolston, Phys. Rev. Lett. **85**, 318 (2000).

[7] T. C. Killian, M. J. Lim, S. Kulin, R. Dumke, S. D. Bergeson, and S. L. Rolston, Phys. Rev. Lett. **86**, 3759 (2001).

[8] F. Robicheaux and J. D. Hanson, Phys. Rev. Lett. **88**, 055002 (2002).

[9] F. Robicheaux and J. D. Hanson, Phys. Plasmas **10**, 2217 (2003).

[10] T. Pohl, T. Pattard, and J. M. Rost, Phys. Rev. A **68**, 010703(R) (2003).

[11] S. Mazevet, L. A. Collins, and J. D. Kress, Phys. Rev. Lett. **88**, 055001 (2002).

[12] S. G. Kuzmin and T. M. O'Neil, Phys. Plasmas **9**, 3743 (2002).

[13] M. S. Murillo, Phys. Rev. Lett. **87**, 115003 (2001).

[14] M. P. Robinson, B. Laburthe Tolra, M. W. Noel, T. F. Gallagher, and P. Pillet, Phys. Rev. Lett. **85**, 4466 (2000).

[15] S. K. Dutta, D. Feldbaum, A. Walz-Flannigan, J. R. Guest, and G. Raithel, Phys. Rev. Lett. **86**, 3993 (2001).

[16] G. Vitrant, J. M. Raimond, M. Gross, and S. Haroche, J. Phys. B **15**, L49 (1982).

[17] A. Walz-Flannigan, J. R. Guest, J.-H. Choi, and G. Raithel, Phys. Rev. A **69**, 063405 (2004).

[18] T. F. Gallagher, P. Pillet, M. P. Robinson, B. Laburthe-Tolra, and M. W. Noel, J. Opt. Soc. Am. B **20**, 1091 (2003).

[19] J. H. Hoogenraad and L. D. Noordam, Phys. Rev. A **57**, 4533 (1998).

[20] W. P. Spencer, A. G. Vaidyanathan, D. Kleppner, and T. W. Ducas, Phys. Rev. A **26**, 1490 (1982).

[21] R. E. Olson, Phys. Rev. Lett. **43**, 126 (1979).

[22] Y. Hahn, J. Phys. B **33**, L655 (2000).

[23] A. L. de Oliveira, M. W. Mancini, V. S. Bagnato, and L. G. Marcassa, Phys. Rev. A **65**, 031401(R) (2002).

[24] W. E. Cooke and T. F. Gallagher, Phys. Rev. A **21**, 588 (1980).